

The lattice Boltzmann method for fluid flow in microchannel and applications

Jiraporn Yojina^{1*}, Wannapong Triampo², Narin Nuttavut², Yongwimon Lenbury¹,
and Phadungsak Ratanadecho³

¹Department of Mathematics, Faculty of Science, Mahidol University
Bangkok 10400, Thailand

Tel: 08-1993-9918, *E-mail: jyojina@yahoo.com

²R&D Group of Biological and Environmental Physics, Department of Physics, Faculty of Science,
Mahidol University, Bangkok 10400, Thailand

Tel: 0-2201-5731, E-mail: wtriampo@gmail.com

³Department of Mechanical Engineering, Faculty of Engineering, Thammasat University (Rungsit
Campus), Klong Luang, Pathemtani 12121, Thailand

Tel: 0-2564-3001, Fax: 0-2564-3010, *E-mail: ratphadu@engr.tu.ac.th

Abstract

The lattice Boltzmann (LB) method based on the D2Q9 model with a single relaxation time is used to simulate the flow field around a square obstacle inside a two-dimensional microchannel. The simulation results are described the dynamical behavior of the flow in a range of Reynolds number between 1 and 300. It is found that this approach enhances the understanding of the flow pattern in highly complex geometries and the results can provide useful information in the design of the realistic model.

Keywords: lattice BGK model, D2Q9, obstacle

1. Introduction

In recent years the lattice Boltzmann method (LBM) has developed efficient numerical tool for simulating fluid flows and transport phenomena based on kinetic equations and statistical physics [1-4]. Typical examples are steady plane Poiseuille flow, thermal viscous cavity flow, multiphase flows and high-speed compressible flows, etc. The success of this method can be partly attributed to the particle based approach which is directly inherited from its predecessor, the lattice gas automata (LGA). Unlike LGA, the LBM simulates a flow system by tracking the evolution of particle distributions instead of tracking single particles. Compared with other traditional computational fluid dynamics method, such as the finite difference schemes, the major advantage of LBM is that it provides a good insight into the underlying microscopic dynamics of the physical system investigated, whereas most methods focus only on the solution of the macroscopic equations [5-7].

The flow through square obstacle in a two-dimensional (2D) channel has been an attraction in all

kinds of fluid mechanical investigations for a long time. Much work has been done in simulating 2D flow around such bluff obstacles in the past. In particular, the 2D flow around circular cylinders has been studied extensively. In contrast to many theoretical, experimental, and numerical data on the flow around circular cylinder over a wide range of Reynolds numbers, there are very few similar studies and information on the flow around square bodies [8-10]. Previous investigations of the flow around circular cylinders performed with the LBM clearly show that this method is an appropriate tool for such kinds of flows [11].

In this work we investigate the flow pattern phenomena and the topology of the vortex structure behind the square obstacle in a 2D microchannel for the range of Reynolds number between 1 to 300.

2. Description of numerical method

For the computations, a 2D 9-bit incompressible lattice-Boltzmann model (D2Q9) with single time Bhatnagar-Gross-Krook (BGK) relaxation collision

operator $\Omega = -\frac{1}{\tau}(f_\alpha - f_\alpha^{(eq)})$ proposed by Bhatnagar,

Gross and Krook [5] is used

$$f_\alpha(x + e_\alpha \delta t, t + \delta t) - f_\alpha(x, t) = \Omega_\alpha \quad (1)$$

where subscript α indicates the velocity direction (α runs from 0 to 8), and δx , δt are the lattice grid spacing and the time step, respectively. The particle speed, c , is defined as $c = \delta x / \delta t$. The dimensionless relaxation time τ

is related to the kinematic viscosity as $\nu = \frac{(2\tau - 1)(\delta x)^2}{6 \delta t}$.

And $f_\alpha(x, t)$ is the density distribution function

associated with the particle at node x and time t with discrete velocity e_α ,

$$e_\alpha = \begin{cases} (0,0), & \alpha=0 \\ c(\cos \theta_\alpha, \sin \theta_\alpha), \theta_\alpha = (\alpha-1)\frac{\pi}{2}, \alpha=1,2,3,4 \\ \sqrt{2}c(\cos \theta_\alpha, \sin \theta_\alpha), \theta_\alpha = (\alpha-5)\frac{\pi}{2} + \frac{\pi}{4}, \alpha=5,6,7,8 \end{cases}$$

And $f_\alpha^{(eq)}(x,t)$ is the corresponding local equilibrium distribution function, which is determined by

$$f_\alpha^{(eq)}(x,t) = \omega_\alpha \rho \left[1 + 3 \frac{e_\alpha \cdot \bar{u}}{c^2} + \frac{9}{2} \frac{(e_\alpha \cdot \bar{u})^2}{c^4} - \frac{3}{2} \left(\frac{\bar{u}}{c} \right)^2 \right] \quad (2)$$

This local equilibrium distribution function has to be computed every time step for every node from the components of the local flow velocity $\bar{u} = (u, v)$, the fluid density ρ , a lattice geometry weighting factor ω_α ,

$$\omega_0 = \frac{4}{9}, \quad \omega_\alpha = \frac{1}{9} \quad \text{for } \alpha=1,2,3,4 \quad \text{and} \quad \omega_\alpha = \frac{1}{36} \quad \text{for } \alpha=5,6,7,8.$$

3. Detail of the test case

The system of interest is a horizontal channel with an obstacle in the form of a square positioned inside it. The problem domain and specified boundary condition are shown in Fig. 1. The size of the obstacle, d , the channel height, H , and an inflow length l , $l = L/5$, define the solid blockage of the confined flow (blockage ratio $\beta = d/H$).

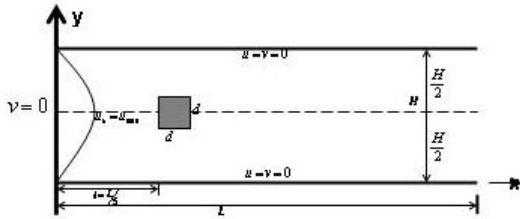


Figure 1. Definition of the geometry and domain.

The dimensionless equations for continuity and momentum may be expressed as

$$\nabla \cdot \bar{u} = 0, \quad (3)$$

$$\frac{\partial \bar{u}}{\partial t} + \nabla \cdot (\bar{u}\bar{u}) = -\nabla p + \frac{1}{\text{Re}} \nabla^2 \bar{u} \quad (4)$$

where $\text{Re} = \frac{u_{\max} d}{\nu}$ is the Reynolds number, u_{\max} is the maximum flow velocity of the parabolic inflow profile and ν is the kinematic viscosity.

The boundary conditions in this investigation are as follow. At the inlet, a parabolic velocity inflow profile is applied. The outflow boundary condition for velocity is

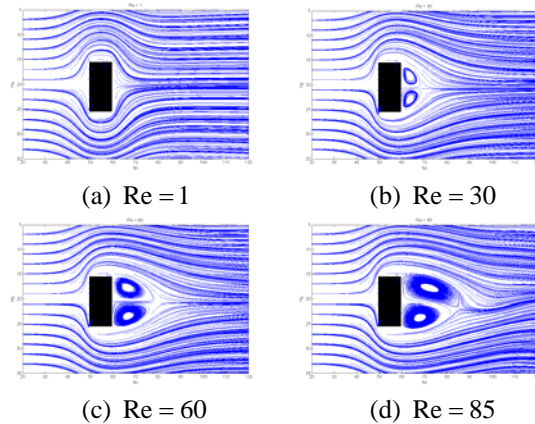
$\frac{\partial u}{\partial x} = \frac{\partial v}{\partial x} = 0$. No-slip boundary conditions are prescribed at the body surfaces. At the top and bottom surfaces of the channel, symmetry conditions simulating a frictionless wall are used ($u = v = 0$).

4. Results and discussion

A Reynolds number range $1 \leq \text{Re} \leq 300$ was investigated numerically on a 40×250 lattice. For all cases considered, the channel length and width were set to 250 and 40 respectively, and the obstacle size 10×10 in lattice unit was positioned at $l = L/5$ downstream the entrance of the channel. The blockage ratio was fixed at $\beta = 1/4$. The following section starts with a description of the different flow patterns observed with increasing Re . Furthermore, the computations are analyzed flow parameter as Strouhal number.

4.1 Flow pattern

Fig. 2. shows computational results by streamline plot at different Reynolds numbers ($\text{Re} = 1, 30, 60, 85, 100, 200$), each characterizing a totally different flow regime. At low $\text{Re} \leq 1$, the creeping steady flow past the square obstacle persists without separation (Fig. 2(a)). A steady recirculation region of two symmetrically placed vortices on each side of the wake, as shown in Fig. 2(b)-2(c), whose length grows as Re increases. The steady, elongated and closed near-wake becomes unstable when $\text{Re} > \text{Re}_{crit}$ (Fig. 2(d)-2(f)). The value $\text{Re}_{crit} \approx 85$ was observed in the present computations. When Re is further increased as shown in Fig. 3. This phenomenon is well known as the von *von Ka'rma'n vortex street*, the wavelength of vortex shedding decreases with rising Re . Another important change in the flow structure is observed in the range $\text{Re} = 86$ to 300, where separation already starts at the leading edge of the square obstacle. As will be see below, this strongly influences the frequency of vortex shedding.



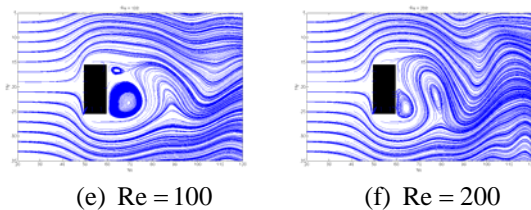


Figure 2. Streamlines plot around the square obstacle for different numbers.

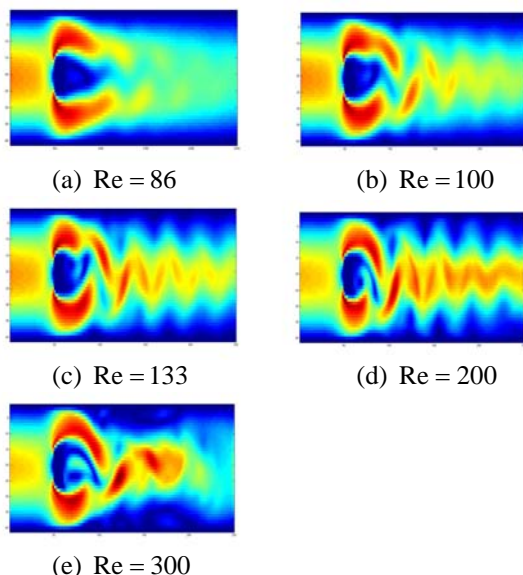


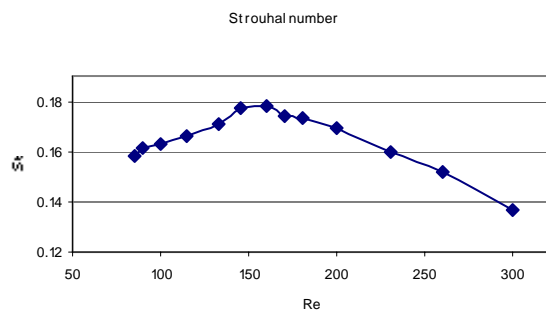
Figure 3. Velocity profiles around the square obstacle for different numbers.

4.2 Strouhal number

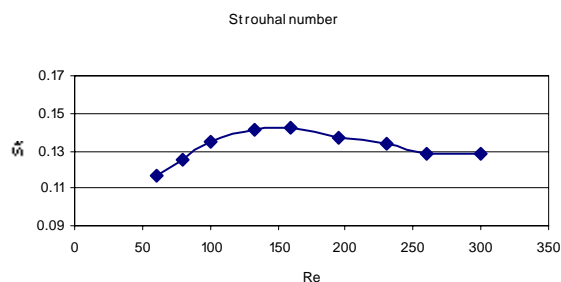
One important quantity taken into account in the present analysis is the strouhal number, St , computed from the obstacle size d , the measured frequency of the vortex shedding f and the maximum velocity u_{max} at the inflow

$$St = \frac{fd}{u_{max}} \quad (5)$$

The characteristic frequency f was determined by a spectral analysis of time series of the temporal evolution of u-component of the flow velocity at several points in the wake behind the obstacle. The simulations show an increase in the strouhal number with increasing Re . The Strouhal number has a maximum at about $Re = 160$ and decreases again for higher Re while Guo *et al.* found a similar curve to that in the present investigation with a maximum at $Re \approx 160$ as shown in Fig. 4.



(a)



(b)

Figure 4. Comparison of computed Strouhal number St for different Reynolds number with data form the literature. (a) present work ($\beta = 0.25$); (b) Guo *et al.* ($\beta = 0.125$).

5. Conclusion

In order to generate reliable numerical results, a newly developed incompressible uniform lattice-BGK model was applied to investigate that 2D flow around a square obstacle inside a channel ($\beta = 0.25$) in the Reynolds number range $1 \leq Re \leq 300$. We have shown that our implementation of the lattice-BGK approach yields reliable results. For steady flow ($Re < 85$), the results was found for the length of recirculation region. The unsteady flow computations demonstrate the capability of the LBA to deal with instantaneous flows. Strouhal numbers were determined for the Reynolds number range ($Re > Re_{crit}$). Finally, this method provide a local maximum of St at $Re \approx 160$. We will further use this method to simulate with increasing complexity of the obstacle structure and become highly complex structures.

Acknowledgment

We would like to thank the many colleagues who contributed in different manners to this work. This work was supported by the Development Promotion of Science and Technology (DPST).

References

1. G. McNamara, and G. Zanetti, 1988. Use of the Boltzmann equation to simulate lattice-gas automata. *Physical Review Letters*, Vol. 61, pp. 2332-2335.
2. S. Chen, H. Chen, D. Martinez, and W. Matthaeus, 1991. Lattice Boltzmann model for simulation of

- magnetohydrodynamics. *Physical Review Letters*, Vol. 67, pp. 3776-3779.
3. H. Chen, S. Chen and W. Matthaeus, 1992. Recovery of the Navier-Stokes equations using a lattice-gas Boltzmann method. *Physical Review A*. Vol. 45, pp. R5339.
 4. Y. Qian, D. D’Humières and P. Lallemand, 1992. Lattice BGK models for Navier-Stokes equation. *Europhysics Letters*. Vol. 17, pp. 479-484.
 5. P.L. Bhatnagar, E. P. Gross and M. Krook, 1954. A model for collision Processes in Gases. I. Small Amplitude Processes in Charged and Neutral One-Component Systems. *Physical Review*. Vol. 94, pp. 511.
 6. X. He, and L. S. Luo, 1997. A priori derivation of the lattice Boltzmann equation. *Physical Review E*, Vol. 55, pp. R6333.
 7. X. He, and G. D. Doolen, 1997. Lattice Boltzmann method on a curvilinear coordinate system: Vortex shedding behind a circular cylinder. *Physical Review E*, Vol. 56, pp. 434.
 8. M. Breuer, J. Bernsdorf, T. Zeiser, and F. Durst, 2000. Accurate computations of the laminar flow past a square cylinder based on two different methods: lattice-Boltzmann and finite-volume. *International Journal of Heat and Fluid Flow*, Vol. 21, pp. 186-196.
 9. G. W. Bin, W. N. Chao, S. B. Chang, and G. Z. Li, 2003. Lattice-BGK simulation of a two-dimensional channel flow around a square cylinder, *Chinese Physics*, Vol. 12, pp. 67-74.
 10. P. Ratanadecho, 2003. Practical Aspect of the Simulation of Two-Dimensional Flow Around Obstacle with Lattice Boltzmann method (LBM), *Thammasat international Journal of Science and Technology*, Vol. 8, pp. 27-35.
 11. J. Latt, and B. Chopard, 2006. Lattice Boltzmann method with regularized pre-collision distribution functions, *Mathematics and Computers in Simulation*, Vol. 72, pp. 165-168.